

## Unsaturated cryptophanes: toward dual PHIP/hyperpolarised xenon sensors

Gaspard Huber, Estelle Léonce, Orsola Baydoun, Nicolas De Rycke, Thierry  
Brotin, Patrick Berthault

► **To cite this version:**

Gaspard Huber, Estelle Léonce, Orsola Baydoun, Nicolas De Rycke, Thierry Brotin, et al.. Unsaturated cryptophanes: toward dual PHIP/hyperpolarised xenon sensors. *Magnetic Resonance in Chemistry*, Wiley, In press, 56, pp.672-678. <<http://onlinelibrary.wiley.com/wo1/doi/10.1002/mrc.4691/abstract>>. <10.1002/mrc.4691>. <cea-01660523>

**HAL Id: cea-01660523**

**<https://hal-cea.archives-ouvertes.fr/cea-01660523>**

Submitted on 11 Dec 2017

**HAL** is a multi-disciplinary open access archive for the deposit and dissemination of scientific research documents, whether they are published or not. The documents may come from teaching and research institutions in France or abroad, or from public or private research centers.

L'archive ouverte pluridisciplinaire **HAL**, est destinée au dépôt et à la diffusion de documents scientifiques de niveau recherche, publiés ou non, émanant des établissements d'enseignement et de recherche français ou étrangers, des laboratoires publics ou privés.

# Unsaturated cryptophanes: toward dual PHIP/hyperpolarised xenon sensors

Gaspard Huber,<sup>1</sup> Estelle Léonce,<sup>1</sup> Orsola Baydoun,<sup>2</sup> Nicolas De Rycke,<sup>2</sup>  
Thierry Brotin,<sup>2</sup> Patrick Berthault\*<sup>1</sup>

1. NIMBE, CEA, CNRS, Paris-Saclay University,  
CEA Saclay, 91191 Gif-sur-Yvette, France

2. Lyon 1 University, Ecole Normale Supérieure de Lyon, CNRS UMR 5182, laboratoire de  
Chimie, 69364 Lyon, France

## Abstract

Cryptophanes, cage-molecules constituted of aromatic bowls, are now well recognized as powerful xenon hosts in  $^{129}\text{Xe}$  NMR-based biosensing. In the quest of a dual probe that can be addressed only by NMR we have studied three cryptophanes bearing a tether with an unsaturated bond. The idea behind this is to build probes that can be detected both *via* hyperpolarised  $^{129}\text{Xe}$  NMR and Para-Hydrogen Induced Polarisation (PHIP)  $^1\text{H}$  NMR. Only two of the three cryptophanes experience a sufficiently fast hydrogenation enabling the PHIP effect. While the in-out xenon exchange properties are maintained after hydrogenation, the chemical shift of xenon encaged in these two cryptophanes is not strikingly modified, which impedes safe discrimination of the native and hydrogenated states *via*  $^{129}\text{Xe}$  NMR. However, a thorough examination of the hyperpolarised  $^1\text{H}$  spectra reveals some interesting features for the catalytic process and gives us clues for the design of doubly smart  $^1\text{H}/^{129}\text{Xe}$  NMR-based biosensors.

## INTRODUCTION

In the seek for sensitive sensors of chemical or biochemical events, NMR molecular probes have a special role as this modality enables investigation in deep tissues and in a non-invasive way. In this field, the recent use of hyperpolarised species, remedying the intrinsic lack of sensitivity of NMR, opens new perspectives.

At the present time, it is widely recognized that dual sensors such as those involving PET/NMR<sup>[1]</sup> or fluorescence/NMR<sup>[2][3][4]</sup> have a great potential. Furthermore, if the

molecular probes are revealed through the same modality the approach constitutes an effective means to obtain a wider viewing angle at a minimum cost.

The present work aims at studying several molecular systems which are precursors of a new generation of purely NMR dual sensors. Their structure is composed of two parts: a cage-molecule able to reversibly host xenon and which can further be decorated by chemical or biological ligands, and a group containing an unsaturated bond where hydrogenation will occur. The former part will enable enhanced detection via hyperpolarised  $^{129}\text{Xe}$  NMR owing to the in-out xenon exchange, the second part will be detected by the PHIP (Para-Hydrogen Induced Polarisation) method.<sup>[5]</sup> Therefore, a dual detection will be possible on the same NMR spectrometer using a commercial probe head. While  $^{129}\text{Xe}$  NMR will hardly give direct information on the sensor structure (except maybe through SPINOE experiments <sup>[6]</sup>),  $^1\text{H}$  NMR with enhanced sensitivity afforded by the use of para-hydrogen will complete the picture and hopefully give precious information on the conformational and kinetics behaviour of the compounds in solution.

After addition on these precursors of a tether for recognition of given molecular targets, the resulting sensors are intended to be detected both *via*  $^1\text{H}$  NMR immediately after hydrogenation with para-hydrogen (density-based contrast) and *via* hyperpolarized  $^{129}\text{Xe}$  NMR. For the latter, the chemical shift of xenon caged in the cryptophane is expected to be modified when the sensor reaches the target, leading to the concept of activatable (or smart) probe.<sup>[7]</sup> As the group containing the unsaturated bond is modified upon hydrogenation, it is important (but not mandatory) that the caged xenon chemical shift also reflects this modification of the host molecule. This is a criterion we have chosen in this study.

## RESULTS

In this study, three cryptophane cores of close structure differing only by the length of the linkers joining cyclotrimeratrylene bowls and bearing a non-conjugated double bond have been used comparatively. They are depicted in Figure 1.

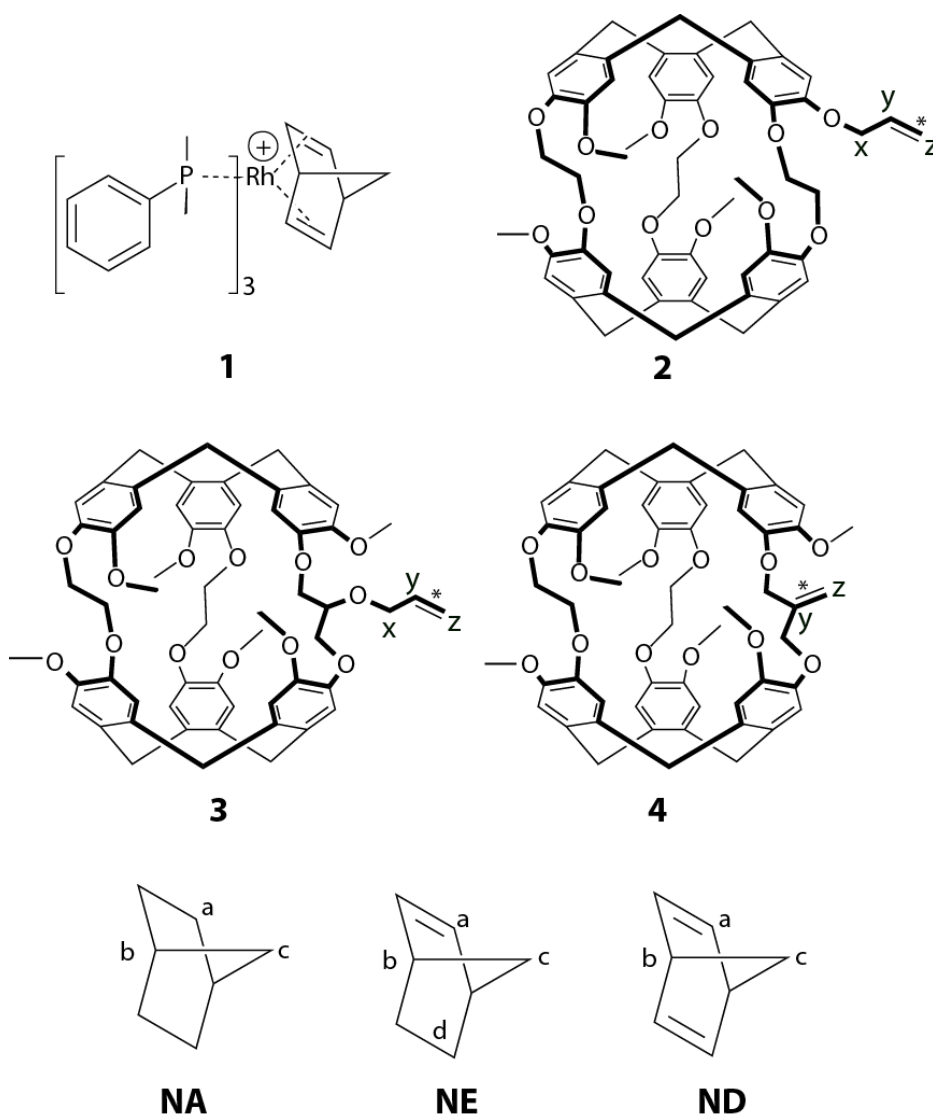


**Figure 1.** Compounds used in this study. Cryptophanes **2h**, **3h** and **4h** correspond to cryptophanes **2**, **3** and **4**, respectively, after hydrogenation of the double bond noted by a star. **1** is the catalyst used in this study. **NA**: norbornane; **NE**: norbornene; **ND**: norbornadiene.

Compound **2** is the cryptophane precursor of the cryptophanol-A, which has been used as an intermediate for the synthesis of numerous  $^{129}\text{Xe}$  NMR-based biosensors.<sup>[8][9][10]</sup> It belongs to the first generation of cryptophane derivatives where the ligand is attached directly on one aromatic ring. Compounds **3** and **4** belong to a second-generation of cryptophane derivatives in which the ligand is tethered on the propylenedioxy linker of a cryptophane-223 core.<sup>[11]</sup> Compound **3** has been prepared to solve the purification problems of the biosensors inherent to the synthesis of **2**. This new strategy represents numerous assets for the synthesis of biosensors. For

instance, this compound gives us the possibility to attach other reactive functions different from the ones attached on the benzene rings. This is a major asset for the construction of more elaborated molecules. Compound **4** is a new derivative used for building new  $^{129}\text{Xe}$  NMR-based biosensors. Its synthesis has not been reported yet in the literature (see its characterization in Figs. S1, S2 and S3 of the Supp. Info.). Thanks to the presence of the non-conjugated double bond, new chemical functions would be easily added on the cryptophane backbone. They can also be used to introduce new ligands of biological interest. This compound has been prepared in moderate yield and the synthesis of this compound will be reported in due course.

The three cryptophanes have been dissolved in 1,1,2,2-tetrachloroethane- $d_2$  at the same concentrations. This solvent has been chosen as i) it is too big to enter in the cryptophane cavity,<sup>[12][13]</sup> ii) the solubility of di-hydrogen is rather high (no data has been found for solubility in tetrachloroethane, but it can be assumed that the solubility properties of xenon in dichloromethane and tetrachloroethane are very similar, i.e. 3.5 mM under 1 bar at 298K <sup>[14]</sup>), iii) PHIP experiments have already been performed in chlorinated solvents.<sup>[15]</sup> The use of more popular solvents such as methanol or acetone could have been chosen, as the solubility of di-hydrogen is probably higher, but at the risk that they enter the cryptophane cavity.

The choice of the catalyst has been dictated by its efficiency for the PHIP experiments. Various organo-soluble hydrogenation catalysts have been tested in preliminary experiments, among which Crabtree's catalyst,<sup>[16]</sup> Wilkinson's catalyst,<sup>[17]</sup> and [1,4-bis(diphenylphosphino)butane](1,5-cyclooctadiene)rhodium(I) tetrafluoroborate.<sup>[18]</sup> Our choice has been oriented towards the commercial catalyst [tris(dimethylphenylphosphine)] (2,5-norbornadiene) rhodium(I) hexafluorophosphate ([Rh(nor)(tdmpp)]PF<sub>6</sub>, compound **1** in Figure 1) because of the far higher hydrogenation turnover rate induced on considered cryptophanes. This agrees with results from Roth who compared the efficiency of seven catalysts for PHIP experiments.<sup>[19]</sup> Compound **1**, the only one among the catalysts tested bearing a norbornadiene group instead of a cyclooctadiene group as a protecting ligand, has been found the most active one.

For the PHIP experiments, the same quantity of catalyst **1** has been introduced in each tube.

Firstly, laser-polarised  $^{129}\text{Xe}$  NMR experiments have been performed on these compounds in similar experimental conditions. In simple one-scan 1D experiments, after having referenced the signal of xenon free in the solvent at 224 ppm (the tetrachloroethane protons resonate at 6 ppm), the caged xenon chemical shifts appear at 68.8, 58.4 and 64.1 ppm for xenon in compounds **2**, **3** and **4**, respectively (see Table 1). It is worth noting that the signals of Xe@**2** and Xe@**3** appear in a spectral region which correspond to what is expected for a cryptophane-222 derivative and a cryptophane-223 derivative, respectively, whereas Xe@**4** experiences a downfield shift, likely due to the anisotropy cone of the double bond, spatially close to caged xenon.

Fast repetitions of the sequence [frequency-selective excitation centred à 60 ppm - acquisition] performed in 2D have enabled us to ensure that a xenon in-out exchange, on the order of 30 Hz, is present. Experiments with and without catalyst in the tubes have shown that this rate is not modified, which indicates that the catalyst does not enter in the cryptophane cavities (this is confirmed by  $^1\text{H}$  experiments revealing no modification of the cryptophane signals upon addition of **1**). This is a prerequisite for obtaining powerful  $^{129}\text{Xe}$  NMR-based biosensors for which the xenon in-out exchange leads to enhanced sensitivity.

Compound	$\delta^{129}\text{Xe}$ (ppm)	Compound	$\delta^{129}\text{Xe}$ (ppm)
<b>2</b>	68.8	<b>2h</b>	68.3
<b>3</b>	58.4	<b>3h</b>	58.7
<b>4</b>	64.1	<b>4h</b>	56.7

**Table 1.** Chemical shifts of xenon encapsulated in the cryptophanes before and after their hydrogenation, at 297 K.

PHIP experiments have then been performed in the same conditions on the cryptophane samples. As in our protocol para-hydrogen ( $p\text{-H}_2$ ) is introduced at a pressure of 4 bar (see Experimental), we could keep xenon (at a sub-atmospheric pressure on top of the solution) in the NMR tube. This ensures that the cryptophanes do not take only an imploded form.<sup>[20][21]</sup>

Immediately after introduction of p-H<sub>2</sub>, successive 1D <sup>1</sup>H spectra have been recorded. Figure 2 displays the high field region of the spectra (full spectrum in Figure S4 of the Supp. Info.) immediately after introduction of p-H<sub>2</sub> (Fig. 2a) and 6 minutes later (Fig. 2b). Some signals are largely enhanced and have an opposite phase, proving the PHIP phenomenon.

Despite the lack of scalar connectivity between the cryptophane part and the double bond, the presence of the catalyst signals on the spectra, and the poor difference between the aromatic resonance frequencies, <sup>1</sup>H and <sup>13</sup>C assignment of the cryptophane signals before and after hydrogenation has been achieved.

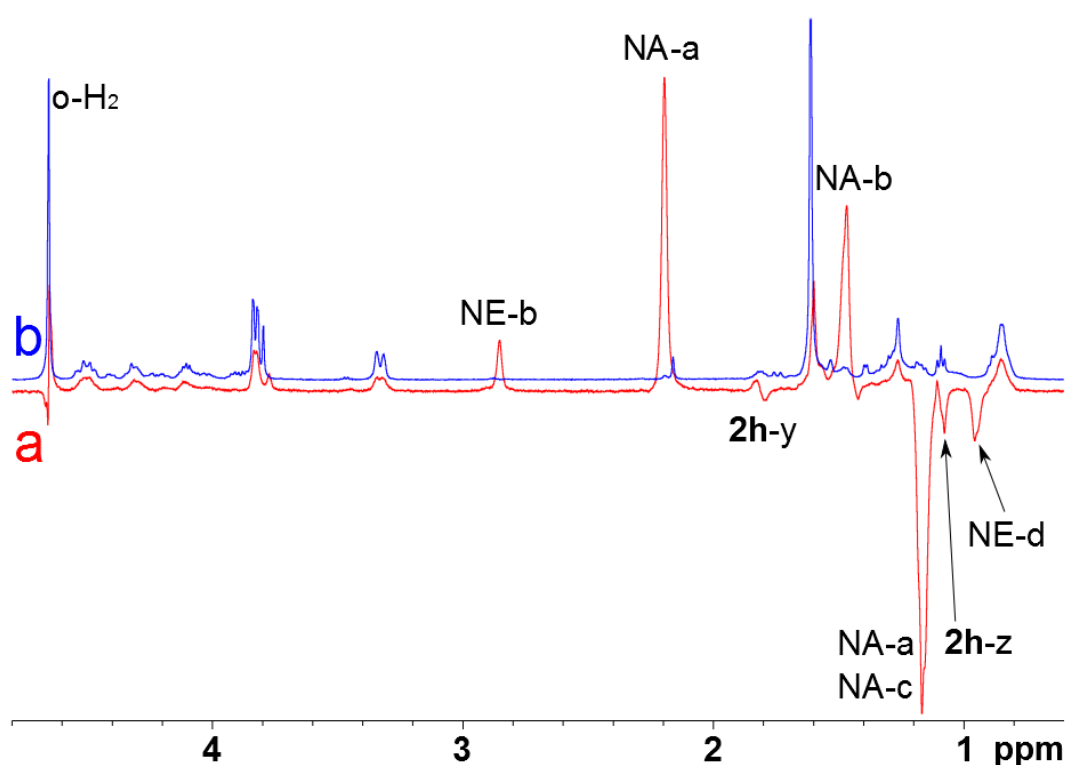


**Figure 2.** Upfield region of the one-scan <sup>1</sup>H NMR spectrum of **2h** (1 mM) in the presence of **1** (0.3 mM), (a) after the introduction of para-hydrogen and (b) 6 minutes later. A 45° readout pulse has been used.

The signal enhancement factors  $\epsilon$  have been estimated to 68, 15 and -42 for protons a, b and c of norbornane by comparing the spectra of Figure 2. Modest enhancement factors between 2 and 3 have been estimated for antiphase signals assigned to

protons y and z of **2h**. The  $^1\text{H}$  spectra recorded for cryptophanes **3** and **4** after addition of para-hydrogen are given in Supporting Information (Figures S5 and S6 for **3h** and **4h**, respectively).

While the behaviour of **3** at first glance looks like this of **2** with the same profile of negative and positive hyperpolarised peaks, for **4** the situation is totally different: no drastic transient change appears on the cryptophane proton signals.

As the catalyst is activated in the presence of di-hydrogen, its norbornadiene part being transformed into norbornene and then into norbornane, we have decided to perform a PHIP experiment in the presence of the catalyst alone (without cryptophane). Figure 3 displays the  $^1\text{H}$  spectrum obtained just after addition of para-hydrogen in a solution containing the catalyst **1**, and 6 minutes later.

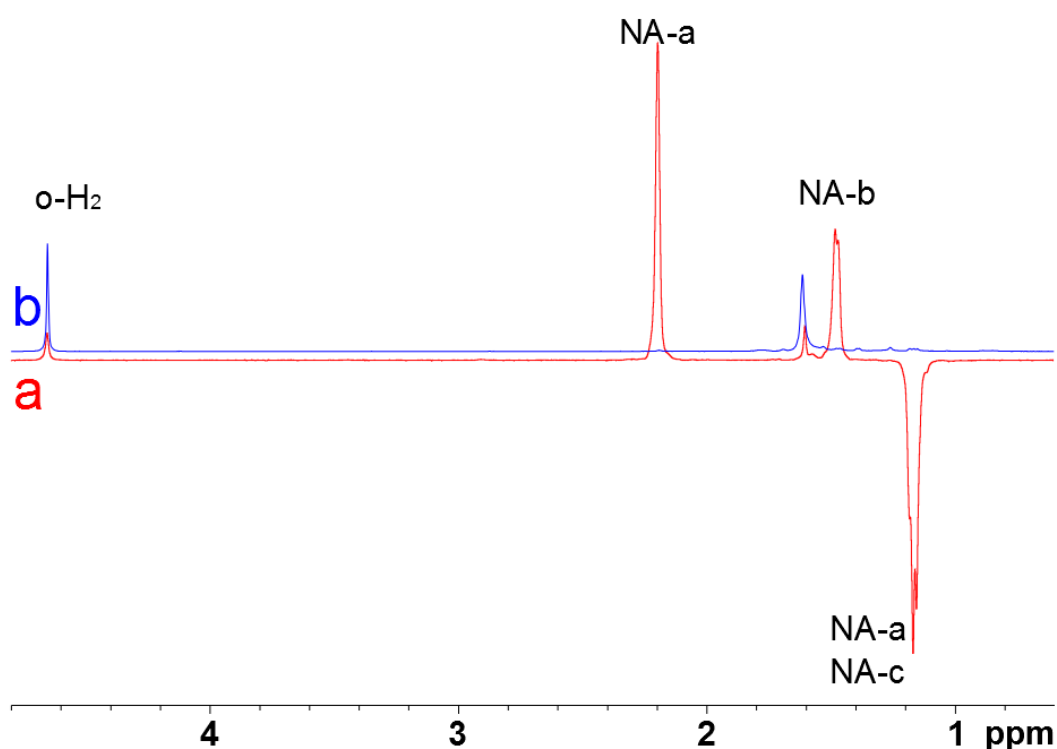


**Figure 3.** Upfield region of the one-scan  $^1\text{H}$  NMR spectrum of **1** (0.3 mM), (a) after introduction of para-hydrogen and (b) 6 minutes later. A  $45^\circ$  readout pulse has been used.



Looking at the difference between the PHIP-hyperpolarised spectrum of **1** and this of the mixture (**2h** + **1**) reveals some signals of the cryptophane which are hyperpolarised. It is worth noting that the signal at 0.95 ppm has been identified as belonging to the norbornene moiety (Figure S7 of the Supp. Info.). Surprisingly this signal does not appear when **1** is hydrogenated, which suggests a particular mechanism when the cryptophane **2** or another molecule bearing a double bond like norbornene, is also present (see the Discussion part). All in all, as long as **2h** is concerned, only the two signals corresponding to the hydrogenated bond, at 1.08 ppm and 1.81 ppm, are hyperpolarised. They appear in antiphase, revealing a PASADENA ("Parahydrogen and Synthesis Allows Dramatically Enhanced Nuclear Alignment") process.<sup>[22]</sup> In order to check this hypothesis, an OPSY ("Only Para-hydrogen SpectroscopY") experiment has been performed.<sup>[23]</sup> The resulting spectrum, displayed in Figure 4, effectively reveals these signals.

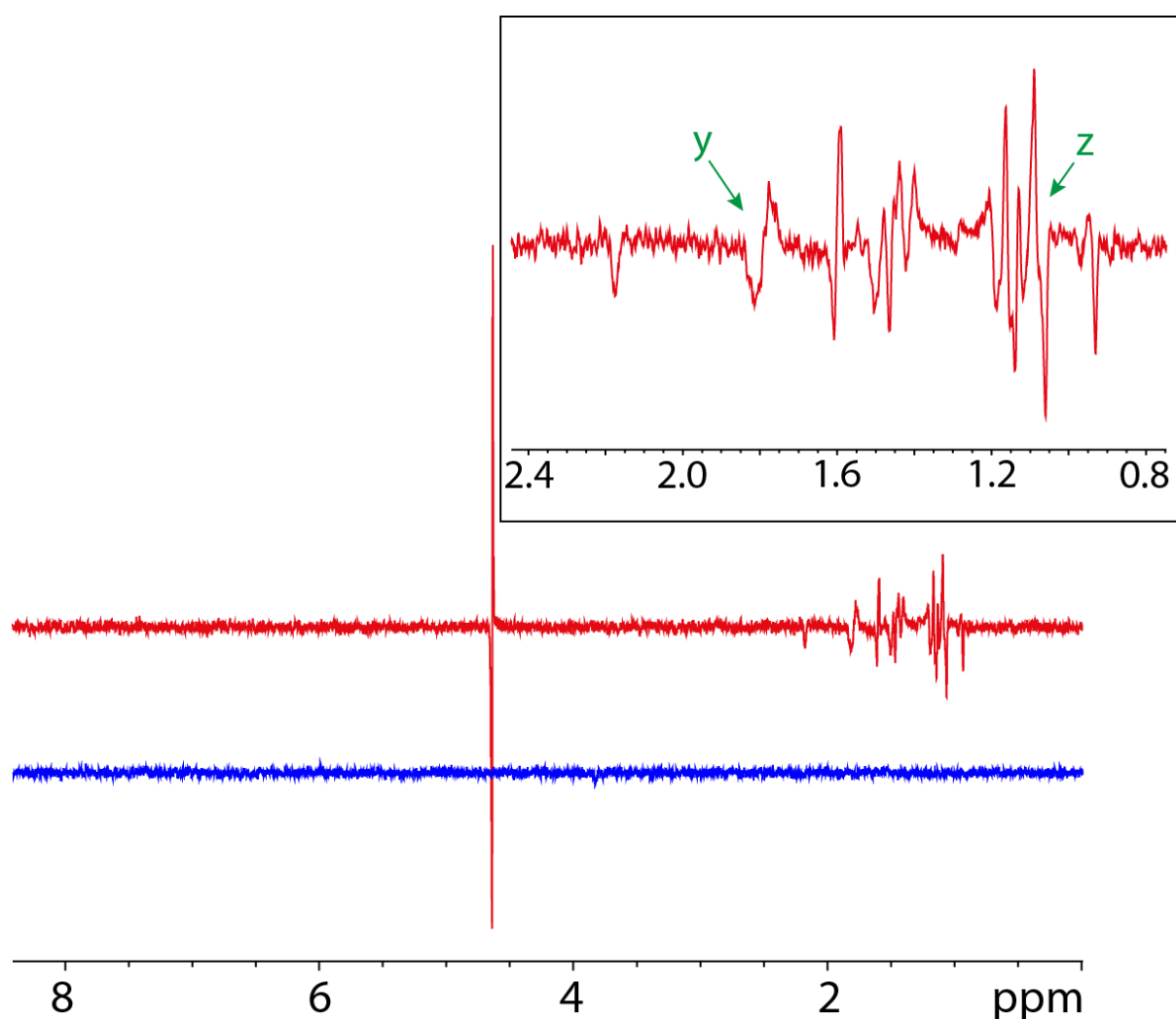


**Figure 4.** OPSY experiment on a sample of **2** at 1 mM and **1** at 0.3 mM (red spectrum). In blue, the same experiment performed on the sample before addition of para-hydrogen.

For compound **3**, the situation is less clear, the cryptophane protons in positions x, y and z resonating at frequencies very close to those of the catalyst. For **4**, the hydrogenation is not fast enough to enable PHIP hyperpolarisation.

Using the gradual disappearance of the signals in z position of **2** and **4**, and the emergence of the methyl signal in z position of **3h**, we have monitored the kinetics of the hydrogenation reaction. Table 2 summarizes the characteristics of the hydrogenation processes for a catalyst concentration of 0.3 mM and a cryptophane concentration of 1 mM. The kinetics data are reported in Figures S8-S10.

Compound	Initial rate (min <sup>-1</sup> )	half-hydrogenation time (min)
<b>2</b>	1.0 at 297K	0.8
<b>3</b>	0.09 at 297K	50
<b>4</b>	0.00093 at 337K	not reached

**Table 2.** Kinetics of the hydrogenation process for compounds **2**, **3** and **4**.

The hydrogenation rate is far lower for cryptophane **4** than for the two other cryptophanes, which explains that no efficient PHIP process is observed for this compound. This is not surprising as it is known that hydrogenation of branched alkenes is slower.

The third step has been to record hyperpolarised <sup>129</sup>Xe NMR spectra on the cryptophanes after hydrogenation. In this purpose, the NMR tubes have been degassed (removal of hydrogen and xenon) before introduction of the hyperpolarised noble gas. For each cryptophane, as before hydrogenation, a signal witnessing xenon inside the molecule-cage is observed in addition to the signal of xenon free in the solvent. The chemical shift values for caged xenon are given in Table 1. Hydrogenation of **2** (leading to compound **2h**) gives rise to an upfield shift by only 0.5 ppm; that of **3** (leading to compound **3h**) a downfield shift of 0.3 ppm. Remarkably the caged xenon chemical shift is upfield shifted by 7.4 ppm when **4** is hydrogenated in **4h** (Figure 5).

Experiments performed at 277K show that this difference is almost conserved while temperature is varying. The xenon linewidths in **4** and **4h** can directly be compared on the same spectrum. The xenon signal inside **4h** is sharper by about 40% than the corresponding signal of xenon inside **4** in the 277-327 K temperature range. This can be interpreted by a higher residence time of xenon in **4h**, in which the methyl group may impede more efficiently the exit of xenon than the vinyl moiety in **4**.

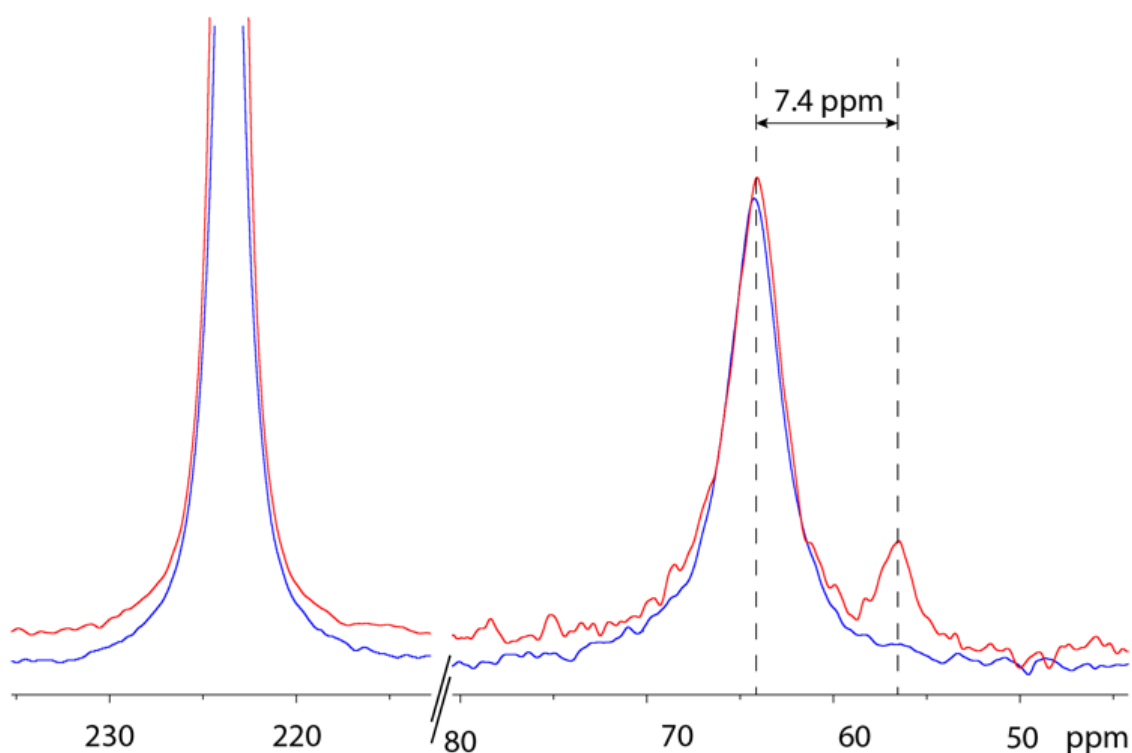


**Figure 5.**  $^{129}\text{Xe}$  NMR spectra before, in blue, and after, in red, partial hydrogenation of **4**. A line broadening of 80 Hz has been applied prior to Fourier transformation.

## DISCUSSION

Joint analysis of the  $^{129}\text{Xe}$  and  $^1\text{H}$  NMR spectra recorded before and after the addition of para-hydrogen indicates that none of these cryptophane derivatives has the qualities required to constitute a bimodal and doubly smart  $^1\text{H}$ - $^{129}\text{Xe}$  NMR probe. By the term 'doubly smart' it is meant a molecular system for which both the  $^{129}\text{Xe}$  and  $^1\text{H}$  NMR spectra are strikingly modified upon addition of para-hydrogen. Here either the caged  $^{129}\text{Xe}$  chemical shift variation after hydrogenation is poor with respect to the line width

(case of compounds **2** and **3**) or hydrogenation is too slow to take profit of the PHIP effect (compound **4**). However, compounds **2** and **3** undoubtedly constitute bimodal probes with interesting and improvable NMR properties. Also a detailed exploration of the spectra of two of these systems reveals interesting features of the hydrogenation, shedding light on the process.

The chemical shifts of xenon in **2h** and **3h** differ from those in **2** and **3**, respectively, by 0.5 ppm at most. This value is small when compared with other cryptophane-based systems. For instance, xenon in a cryptophane bearing a nitrilotriacetic function experiences a more significant chemical shift variation when the molecule chelates some dications.<sup>[24][25]</sup> As an example, the presence of lead cations is translated into a large xenon chemical shift variation of 4.5 ppm. The high conformational dynamics that the allyl arm of **2** may adopt probably explains the partial averaging of the effect of the anisotropy cone of the double bond and thus the small effect on the caged xenon chemical shift when compared to **2h**, lacking this double bond. This also tends to indicate that the allyl arm has negligible influence on the conformation of the cage itself. The difference between the chemical shifts for xenon caged in **3** and in **3h** may also be explained with the same arguments. On the contrary, the non-conjugated double bond of **4** is much less mobile and induces a higher effect on the caged xenon chemical shift, an effect reinforced by the shorter average distance between xenon and the double bond.

The fact that the two protons on both sides of the double bond experience a PASADENA transfer can be explained by the way the hydrogenation experiment was performed. Introduction of para-hydrogen and shaking of the NMR tube was performed 5 seconds outside the NMR magnet, in a field of ca. 12 mT. Then the tube was inserted in the magnet and the NMR experiment started immediately. The data show that activation of the catalyst by para-hydrogen is a prerequisite for the cryptophane hydrogenation. It is thus likely that this second step occurs mostly at a high field, which is also supported by the hydrogenation kinetics studies, giving rise to a preeminent PASADENA effect. It should be noted that although a large majority of the catalyst signals (**1**, norbornene, norbornane) are in phase (Figure 2), after the OPSY experiment also for these protons some antiphase signals appear (Figure 4), probably because part of the hydrogenation of the catalyst still occurs at high magnetic field.

For compound **3h**, the weakness of the antiphase - PHIP-hyperpolarised - signals of the y and z protons, hardly distinguishable among the catalyst's signals, cannot only be explained by the hydrogenation kinetics. Rather, a thorough investigation via EXSY-spectra has shown that an exchange exists between the signals at 0.95, 1.15 ppm and other signals at -2.74, -2.02 ppm (Figure S11). The unusual chemical shift of these latter signals strongly suggest that they represent a form where the propyl moiety enters the cavity of the cryptophane.

The NMR signal of ortho-hydrogen appears as a superimposition of a classical absorptive in-phase signal and an antiphase signal (see Figure 2a) that should come from a PASADENA effect during the hydrogenation process. This is confirmed in the OPSY experiment. Similarly to previously reported examples,<sup>[27][28][29][30][31]</sup> the hyperpolarisation and the antiphase component of the o-H<sub>2</sub> signal probably arise from addition of para-hydrogen on rhodium, where hydrogen atoms are magnetically inequivalent (A-X system), followed by release of o-H<sub>2</sub> with non-thermal spin population. Transfer between longitudinal spin order ( $2I^A_z I^X_z$ ) and longitudinal polarisations ( $I^A_z$  and  $I^X_z$ ) occurs through chemical shift anisotropy and interference terms, as explained in the case of ruthenium complexes.<sup>[27]</sup> The absence of any signal in the hydride region, at chemical shift lower than 0 ppm might be due to the PASADENA conditions. A short life-time of such intermediates indeed induces weak and large signals,<sup>[27]</sup> partly cancelled by their antiphase character. As this chemical process starts as soon as the sample is shaken at low magnetic field, where ALTADENA conditions usually dominate, a hyperpolarised in-phase signal should occur for o-H<sub>2</sub>. However, the longitudinal relaxation time of o-H<sub>2</sub>, measured independently to 1.4 s in the experimental conditions, is short compared to the time, about 5 s, between shaking the tube and recording the NMR spectrum, inducing a large reduction of the expected hyperpolarised signal.

## CONCLUSION

In this paper, we have explored the feasibility of using a dual probe, based on laser-polarised xenon and proton PHIP NMR, in which both signals may be recorded using the same apparatus. Three molecular systems encompassing a cryptophane core and a non-conjugated double bond have been tested, one of them synthesized for the first

time. None of them reached the two objectives, but all reach, at different extent, one objective.

The difference between the chemical shift of xenon in compound **2** and in compound **2h** (also **3** - **3h**) is not high enough to be a marker of the hydrogenation, so compound **2** cannot be considered as a smart  $^{129}\text{Xe}$  NMR sensor.<sup>[7]</sup> This does not mean that the strategy of incorporating a double bond in the spacer has to be set away. Rather, it is likely that a ligand with a high electron density (aromatic ring for instance) preceding or following such a spacer could allow a significant chemical shift variation for caged xenon before and after hydrogenation.

We could also modify the structure of the probe by grafting, close to the non-conjugated double bond, a very polar functional group dedicated to coordinate the metal catalyst, resulting in acceleration of the hydrogenation of the olefin, and thereby enhancing  $^1\text{H}$  NMR signals that result from the PHIP process.

Finally, the concomitant introduction of hyperpolarised xenon and para-hydrogen in the NMR tube, followed by the simultaneous record of  $^{129}\text{Xe}$  and  $^1\text{H}$  spectra, will allow to observe simultaneously the sample through two complementary and sensitive probes. Di-hydrogen could even be introduced in the optical pumping cell for xenon hyperpolarisation, hopefully giving the right gas mixture for an optimal use of the dual probe. Indeed, in a recent work of Meersmann *et al.*, di-hydrogen replaces molecular nitrogen as buffer gas during optical pumping.<sup>[31]</sup>

## EXPERIMENTAL

### Chemicals

[Tris(dimethylphenylphosphine)](2,5-norbornadiene) rhodium(I) hexafluorophosphate **1**, and the other catalysts were purchased from Sigma-Aldrich. Perdeuterated 1,1,2,2-tetrachloroethane and xenon enriched in isotope 129 at 83% were purchased from EurisoTop.

### Cryptophane synthesis

Cryptophanes **2** and **3** were prepared according to a known experimental procedure. (see ref.<sup>[8]</sup> and <sup>[10]</sup>). The synthesis of **4** has not yet been reported in the literature (to be published).  $^1\text{H}$  NMR and  $^{13}\text{C}$  NMR data are fully consistent with the proposed structures (see Supp. Info.).

### Sample preparation

Each NMR tube was filled with 600  $\mu\text{L}$  of a mixture of catalyst **1** and cryptophane (**2**, **3** or **4**) in 1,1,2,2-tetrachloroethane- $\text{d}_2$ , with respective concentrations of 0.3 mM and 1.0 mM.

### Hyperpolarisation methods

**Xenon Optical Pumping.** Xenon was hyperpolarised via Spin Exchange Optical Pumping (SEOP) in the batch mode, using our home-built setup based on two coupled 30 W laser diodes already described.<sup>[32]</sup> After 5 to 10 minutes of optical pumping, hyperpolarised xenon was separated from helium and nitrogen by condensation in a cold exchanger. Frozen xenon was stored and transported in a glass reservoir immersed in liquid nitrogen in a magnetic field of 300 mT. For the transfer to the NMR tube this reservoir was heated and installed in a vacuum line in the fringe field of the NMR magnet. A hollow NMR spinner enabled us to condensate hyperpolarised xenon on top of the previously degassed solution without freezing the solution. The useful xenon nuclear polarisation was around 0.2.

**Para-hydrogen preparation.** Para-hydrogen was produced according to the procedure and home-built setup described in ref. [33]. Cooling of di-hydrogen to 77 K in the presence of hydrous ferric oxide (Molecular Products, Inc.) resulted in a mixture enriched at 51% in  $p\text{-H}_2$  (this percentage was controlled by using Raman spectroscopy, with an experimental error of 2%). It was transported to a glass container at a pressure of ca. 4 bar; in the absence of paramagnetic impurities, the percentage of  $p\text{-H}_2$  remained stable for several hours. Para-hydrogen was introduced in the NMR tube (gassed under xenon) through a simple transfer line.

### NMR experiments

The NMR experiments were performed on a Bruker Avance II spectrometer operating at a frequency of 500.13 MHz for  $^1\text{H}$  and equipped with an inverse broad band probehead with z-gradient. Unless otherwise stated, experiments were recorded at 297 K, in 5 mm o.d. NMR tubes equipped with Teflon valves from Young Scientific Glassware Ltd.

The tubes were vigorously shaken 5 seconds in the vicinity of the unshielded NMR magnet in a fringe field of ca. 150 and 10 mT, for  $^{129}\text{Xe}$  and  $^1\text{H}$  NMR experiments, respectively, then immediately introduced in the NMR magnet. A stabilization delay of ca. 5 seconds was included prior to acquisition for  $^{129}\text{Xe}$  NMR experiments only, while  $^1\text{H}$  NMR experiments started immediately.

### REFERENCES

- [1] R. T. M. de Rosales, *J. Label. Compd. Radiopharm.* **2014**, *57*, 298–303.
- [2] Z. Kotková, J. Kotek, D. Jiráček, P. Jendelová, V. Herynek, Z. Berková, P. Hermann, I. Lukeš, *Chem. Eur. J.* **2010**, *16*, 10094–10102.
- [3] C. Boutin, A. Stopin, F. Lenda, T. Brotin, J. P. Dutasta, N. Jamin, A. Sanson, Y. Boulard, F. Leteurtre, G. Huber, A. Bogaert-Buchmann, N. Tassali, H. Desvaux, M. Carrière, P. Berthault, *Bioorg. Med. Chem.* **2011**, *19*, 4135–4143.
- [4] N. Kotera, E. Dubost, G. Milanole, E. Doris, E. Gravel, N. Arhel, T. Brotin, J.-P. Dutasta, J. Cochrane, E. Mari, C. Boutin, E. Léonce, P. Berthault, B. Rousseau, *Chem. Commun.* **2015**, *51*, 11482–11484.
- [5] S. Glöggl, J. Colell, S. Appelt, *J. Magn. Reson.* **2013**, *235*, 130–142.
- [6] G. Navon, Y. Q. Song, T. Rõõm, S. Appelt, R. E. Taylor, A. Pines, *Science* **1996**, *271*, 1848–1851.
- [7] E. Mari, P. Berthault, *Analyst* **2017**, *142*, 3298–3308.
- [8] T. Brotin, A. Martinez, J.-P. Dutasta, in *Calixarenes Beyond*, Springer, Cham, **2016**, 525–557.
- [9] M. Darzac, T. Brotin, D. Bouchu, J.-P. Dutasta, *Chem. Commun.* **2002**, 48–49.
- [10] M. M. Spence, E. J. Ruiz, S. M. Rubin, T. J. Lowery, N. Winssinger, P. G. Schultz, D. E. Wemmer, A. Pines, *J. Am. Chem. Soc.* **2004**, *126*, 15287–15294.
- [11] L.-L. Chapellet, J. R. Cochrane, E. Mari, C. Boutin, P. Berthault, T. Brotin, *J. Org. Chem.* **2015**, *80*, 6143–6151.
- [12] A. Collet, J.-P. Dutasta, B. Lozach, J. Canceill, in *Supramol. Chem. — Dir. Synth. Mol. Recognit.*, Springer, Berlin, Heidelberg, **1993**, 103–129.
- [13] T. Brotin, J.-P. Dutasta, *Eur. J. Org. Chem.* **2003**, *2003*, 973–984.
- [14] K. Shirono, T. Morimatsu, F. Takemura, *J. Chem. Eng. Data* **2008**, *53*, 1867–1871.
- [15] M. Plaumann, U. Bommerich, T. Trantzscheil, D. Lego, S. Dillenberger, G. Sauer, J. Bargon, G. Buntkowsky, J. Bernarding, *Chem. - Eur. J.* **2013**, *19*, 6334–6339.
- [16] R. H. Crabtree, K. Fujita, Y. Takahashi, R. Yamaguchi, R. H. Crabtree, in *Encycl. Reag. Org. Synth.*, Ed.: John Wiley & Sons, Ltd, Chichester, UK, **2009**.
- [17] J. A. Osborn, F. H. Jardine, J. F. Young, G. Wilkinson, *J. Chem. Soc. Inorg. Phys. Theor.* **1966**, 1711–1732.
- [18] K. Muennemann, M. Kölzer, I. Blakey, A. K. Whittaker, K. J. Thurecht, *Chem. Commun.* **2012**, *48*, 1583–1585.
- [19] M. Roth, Sensitivity Enhancement in NMR by Using Parahydrogen Induced Polarization, PhD thesis, **2010**.
- [20] S. T. Mough, J. C. Goeltz, K. T. Holman, *Angew Chem Int Ed* **2004**, *43*, 5631–5635.
- [21] G. Huber, T. Brotin, L. Dubois, H. Desvaux, J. P. Dutasta, P. Berthault, *J. Am. Chem. Soc.* **2006**, *128*, 6239–6246.
- [22] C. R. Bowers, D. P. Weitekamp, *Phys. Rev. Lett.* **1986**, *57*, 2645–2648.
- [23] J. A. Aguilar, P. I. P. Elliott, J. López-Serrano, R. W. Adams, S. B. Duckett, *Chem. Commun.* **2007**, 1183–1185.
- [24] N. Kotera, N. Tassali, E. Léonce, C. Boutin, P. Berthault, T. Brotin, J.-P. Dutasta, L. Delacour, T. Traoré, D.-A. Buisson, F. Taran, S. Coudert, B. Rousseau, *Angew. Chem. Int. Ed.* **2012**, *51*, 4100–4103.
- [25] N. Tassali, N. Kotera, C. Boutin, E. Léonce, Y. Boulard, B. Rousseau, E. Dubost, F. Taran, T. Brotin, J.-P. Dutasta, P. Berthault, *Anal. Chem.* **2014**, *86*, 1783–1788.
- [26] S. Aime, W. Dastrù, R. Gobetto, A. Russo, A. Viale, D. Canet, *J. Phys. Chem. A* **1999**, *103*, 9702–9705.



- [27] D. A. Barskiy, K. V. Kovtunov, I. V. Koptug, P. He, K. A. Groome, Q. A. Best, F. Shi, B. M. Goodson, R. V. Shchepin, A. M. Coffey, et al., *J. Am. Chem. Soc.* **2014**, *136*, 3322–3325.
- [28] M. L. Truong, F. Shi, P. He, B. Yuan, K. N. Plunkett, A. M. Coffey, R. V. Shchepin, D. A. Barskiy, K. V. Kovtunov, I. V. Koptug, K. W. Waddell, B. M. Goodson, E. Y. Chekmenev, *J. Phys. Chem. B* **2014**, *118*, 13882–13889.
- [29] V. V. Zhivonitko, V.-V. Telkki, K. Chernichenko, T. Repo, M. Leskelä, V. Sumerin, I. V. Koptug, *J. Am. Chem. Soc.* **2014**, *136*, 598–601.
- [30] C. Terenzi, S. Bouguet-Bonnet, D. Canet, *J. Phys. Chem. Lett.* **2015**, *6*, 1611–1615.
- [31] N. J. Rogers, F. Hill-Casey, K. F. Stupic, J. S. Six, C. Lesbats, S. P. Rigby, J. Fraissard, G. E. Pavlovskaya, T. Meersmann, *Proc. Natl. Acad. Sci.* **2016**, *113*, 3164–3168.
- [32] C. Chauvin, L. Liagre, C. Boutin, E. Mari, E. Léonce, G. Carret, B. Coltrinari, P. Berthault, *Rev. Sci. Instrum.* **2016**, *87*, 016105.
- [33] V. Daniele, F.-X. Legrand, P. Berthault, J.-N. Dumez, G. Huber, *ChemPhysChem* **2015**, *16*, 3413–3417.